

Article

New Functionalized Polycycles Obtained by Photocatalytic Oxygenation Using Mn(III) Porphyrins in Basic Media

Dragana Vuk ¹, Ottó Horváth ^{2,*} and Irena Škorić ^{1,*} 

¹ Department of Organic Chemistry, Faculty of Chemical Engineering and Technology, University of Zagreb, Marulićev trg 19, 10000 Zagreb, Croatia; dvuk@fkit.hr

² Department of General and Inorganic Chemistry, Institute of Chemistry, Faculty of Engineering, University of Pannonia, P.O.B. 158, H-8201 Veszprém, Hungary

* Correspondence: horvath.otto@mk.uni-pannon.hu (O.H.); iskoric@fkit.hr (I.Š.);
Tel.: +36-88-624-000 (ext. 6049) (O.H.); +385-1-4597-241 (I.Š.)

Received: 28 February 2019; Accepted: 22 March 2019; Published: 27 March 2019



Abstract: According to our earlier observations, the products of photocatalytic oxygenations of furan and thiophene derivatives of benzobicyclo[3.2.1]octadiene with anionic and cationic manganese(III) porphyrin at pH = 7 strongly depended on the type and position of the heteroatom in the aromatic ring, as well as the charge of the photocatalyst. Hence, a significant pH increase (to 10) in these systems offered a reasonable tool to affect the diversity and yields of the oxygenation products. They were quantitatively separated by TLC and identified with NMR analyses. The results clearly indicated that the increase of HO[−] concentration, in most cases, considerably changed the product yield, e.g., enhanced it to 70% for the hydroxy-furyl derivative. Accordingly, the selectivity of the oxygenation of the furan compound could be improved in this way. In the case of one thienyl compound, however, even an additional product appeared, while the yields of the products of the other thiophene derivative (with cationic catalyst) decreased to zero, suggesting the application of lower pH for preparative purposes. The pH effects indicate that oxygenation reactions in these systems involve more photochemically generated oxidative agents, e.g., •OH and (P)Mn(V)=O, the role of which is affected by the pH increase in various ways.

Keywords: benzobicyclo[3.2.1]octadienes; furan; Mn(III)porphyrins; pH influence; photocatalytic oxygenation; thiophene

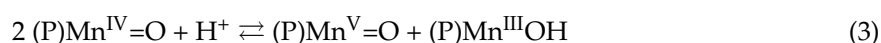
1. Introduction

Several types of porphyrins have been used for photocatalytic oxygenations of various organic compounds. Both free-base ligands and metalloporphyrins proved to be efficient for such reactions. In earlier and more recent works, cycloalkenes were effectively functionalized in such reactions, using porphyrin complexes of various transition metal ions [1–6]. Also, some aromatic (and aliphatic) alcohols and aldehydes were oxidized to carboxylic acids by solar irradiation of a Sb(V)-porphyrin [7]. Photocatalytic oxygenation of cyclohexene was carried out in the system sensitized by Sn(IV)-porphyrin adsorbed on Pt loaded TiO₂ nano-particles [8]. In air- or oxygen-saturated solutions, free-base porphyrins generate only singlet oxygen in these photocatalytic reactions, while metalloporphyrins can be involved in other light-induced processes producing species with higher oxidation potential than that of ¹O₂. Application of manganese(III) porphyrins well demonstrated this diversity. In most of these processes, the first reaction step of the (triplet) excited-state complex was an electron transfer. These reactions produce directly or indirectly Mn(IV) then Mn(V) porphyrins as intermediates playing important roles in the oxygenation processes. This has been exemplified in earlier works [1,9] and more recent studies [10–13],

regarding the photocatalytic oxygenation of cyclohexene. In aqueous systems, photo-induced homolysis of the bond between the metal center and chloride or hydroxide axial ligands led to the formation of (P)Mn^{IV}=O [9,13,14]. The oxidized ligand is a very reactive oxidative agent, e.g., hydroxyl radical in the latter case (Equation (1)). The Mn(II) species formed in this reaction undergoes an oxidation with the dissolved O₂ (Equation (2)).

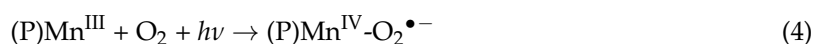


The latter equation is a summary of several steps. The Mn(IV) complexes formed disproportionate, producing highly reactive manganese(V)-oxo species (Equation (3)) [11–13].

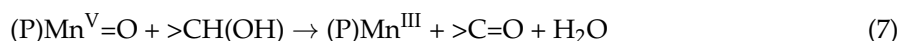
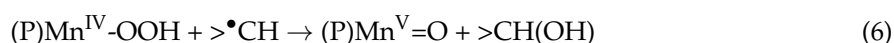


Since disproportionation is significantly faster than the back reaction in this equilibrium system, especially in polar solvent, it is a nearly diffusion-controlled process [11]. Additionally, the rate constants for epoxidation of olefins are several orders of magnitude higher for manganese(V)-oxo porphyrins than for the corresponding Mn(IV) species. Hence, (P)Mn^V=O can be considered as the major oxidant in the photocatalytic oxygenations in these systems. Nevertheless, in some cases, the (P)Mn^{IV}=O complexes can also result in direct hydrogen abstraction from hydrocarbon moiety [15].

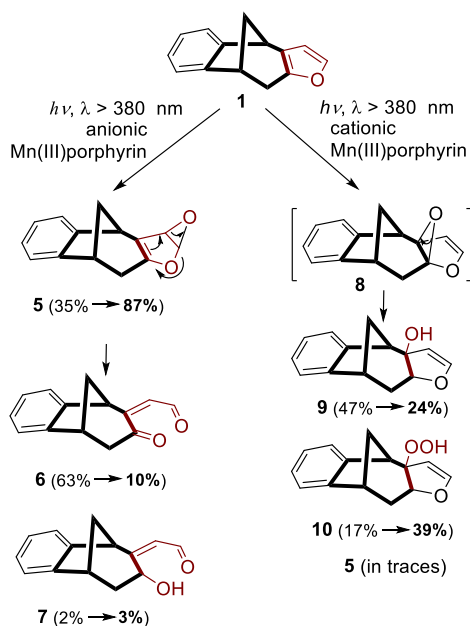
Another photochemical electron transfer in the primary reaction was observed between the excited (triplet) state of the (P)Mn^{III} complex and a dissolved oxygen molecule (Equation (4)) [16].



The putative (P)Mn^{IV} superoxo complex abstracts a hydrogen atom from a saturated hydrocarbon moiety generating a hydroperoxo complex (P)Mn^{IV}-OOH. (Equation (5)). The subsequent reductive O–O bond cleavage by >•CH produces (P)Mn^V=O and >CH(OH) (Equation (6)), followed by the oxidation of >CH(OH) by (P)Mn^V=O to yield >C=O with regeneration of (P)Mn^{III} (Equation (7)).



Manganese(III) porphyrins proved to be efficient photocatalysts for oxygenation reactions, i.e. functionalization, of various derivatives of the benzobicyclo[3.2.1]octadiene skeleton in aqueous systems (in water/acetone (50:50) mixture). In these experiments, Mn(III) complexes with both anionic and cationic porphyrins were utilized, namely 5,10,15,20-tetrakis(4-sulfonatophenyl)porphyrin (Mn(III)TSPP³⁻) and 5,10,15,20-tetrakis(1-methyl-4-pyridinium)porphyrin (Mn(III)TMPyP⁵⁺). Photocatalytic oxygenation of the 2-furyl derivative **1** clearly indicated that the charge of the porphyrin ligand may considerably determine the reaction pathways [17]. As Scheme 1 demonstrates, the cationic catalyst favored the electrophilic attack on the inner double bond of the furan ring, while the negatively charged complex reacted on the outer C=C bond, due to both electronic and steric effects. The more electrophilic positively charged complex, forming (P)Mn^V=O (as in Equation (3)) can more effectively attack a sterically less accessible atom than the corresponding anionic catalyst does. However, if the accessibility of the outer C=C bond became hindered by annulation of a benzene to the outer side of the furan ring, even the negatively charged catalyst could promote oxygenation at the inner positions [18].



Scheme 1. Reaction pathways and product ratios for the photocatalytic oxygenation of **1** under various conditions in air-saturated systems. The arrows in parentheses indicate the change in the yields upon increasing the pH from 7 to 10.

The significant effects of the charge of these photocatalysts were also observed in the photocatalytic oxygenation of different phenyl derivatives of the same skeleton [19]. In that case the substituents on the phenyl ring could also influence the types of the end-products

More interestingly, changes of the position and the type of the heteroatom in the derivatives similar to **1** resulted in considerably (sometimes strikingly) deviating reaction routes under the same experimental conditions [20]. For instance, in the case of a thienyl derivative (**3**, see later in Scheme 4), even the cleavage of the basic skeleton took place. This was the consequence of the higher stability of the thiophene ring, compared to that of the furan ring, due to the significantly stronger aromaticity of the previous one.

Since earlier results with the derivative **1** suggested that a change of pH may considerably affect the ratio (or even the type) of the end-products, and the previous experiments with the other furyl and thienyl derivatives were carried out only in neutral systems (pH = 7), in this work, photocatalytic oxygenation reactions of these derivatives of benzobicyclo[3.2.1]octadiene skeleton were studied in basic media (at pH = 10), by application of both anionic and cationic manganese(III) porphyrins, i.e., (Mn(III)TSPP³⁻) and (Mn(III)TMPyP⁵⁺), in aerated and oxygen-saturated systems. As our new results indicate, this change of pH, combining with the appropriate selection of the charge of the photocatalyst and the starting substrate, offers a suitable possibility for the improvement of the selectivity of these functionalization reactions. For instance, this pH increase dramatically enhanced the yield of the hydroxy-furyl product (from 18–28% to 70%) with both photocatalysts.

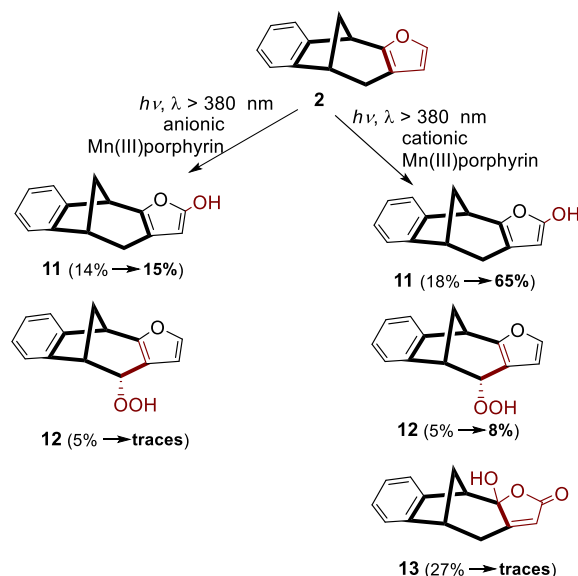
2. Results and Discussion

In this section, the presentation of the experimental results along with their interpretation is organically connected to the corresponding introductory part. Hence, it begins with the photocatalytic oxygenation of another, 3-furyl derivative (**2**) for an easy comparison with the behavior of **1** (see Scheme 1), a constitutional isomer of **2**. In the continuation, the results obtained with the analogous 2- and 3-thienyl derivatives (**3** and **4**) are discussed. Blank experiments were also carried out for all the three starting bicyclo structures **2–4**. No permanent change was observed in the dark (in oxygen-saturated solutions containing both substrate and anionic/cationic catalyst), neither upon

irradiation in the absence of porphyrin. These observations clearly indicated that the substrate does not undergo any thermal reaction even in the presence of ground-state porphyrins.

In the case of the air-saturated system of **2**, the efficiency for the formation of the hydroxy derivative (**11**) was just very slightly affected by the increase of pH from 7 to 10 in the presence of the anionic photocatalyst (Scheme 2). This observation suggests that hydroxylation at an outer position of the furan ring is not promoted by an increase of the HO^- concentration. This observation indicates that an enhanced basicity of the solution hardly decreased the electrophile character of the oxidative agent formed from the anionic catalyst. Regarding the ratio of the peroxo derivative (**12**), although rather moderately changed upon this pH increase, it decreased from 5% to “traces”.

In the presence of the cationic photocatalyst, the pH effects observed for the formation of derivatives **11** and **12** strongly deviate from those with the anionic porphyrin. While pH increase hardly enhanced the ratio of **11** in the latter case, it enormously increased (from 18% to 65%) with the cationic one. This difference suggests that the more basic medium favored the formation of the oxidative agent resulting in the hydroxylation at that outer position. This oxidant is presumably hydroxyl radical because its photoinduced production, according to Equation (1), is promoted by the increased HO^- concentration, due to the more efficient formation of the $(\text{P})\text{Mn}^{\text{III}}\text{OH}$ complex, which is also favored by the highly positive charge of the porphyrin ligand.

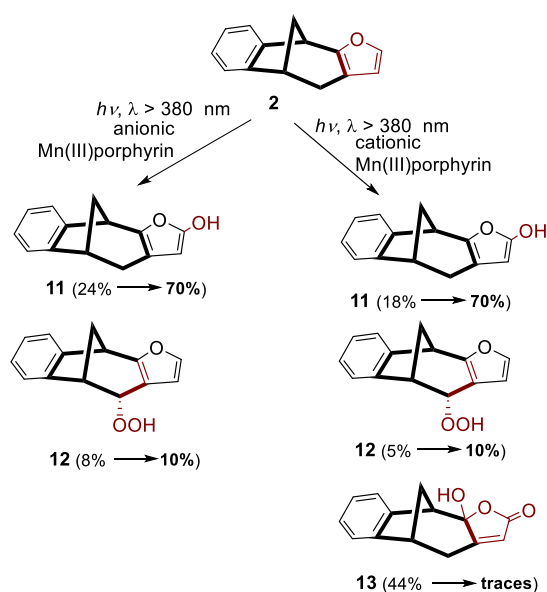


Scheme 2. Reaction pathways and product ratios for the photocatalytic oxygenation of **2** in air-saturated systems. The arrows in parentheses indicate the change in the yields upon increasing the pH from 7 to 10.

For the peroxo derivative (**12**), even the direction of the change in the product yield was just the opposite of that with the anionic catalyst. Instead of an obvious decrease, a modest increase (from 5% to 8%) was observed, in accordance with the result regarding **11**. While in both products the substitution took place at an outer position, in the presence of the cationic catalyst, a third derivative (**13**) with an inner hydroxy group (and a carbonyl in the ring) was also formed. Its yield significantly decreased upon the pH increase (from 27% to traces). These results suggest that the $\text{Mn}^{\text{V}}=\text{O}$ species plays an important role in the formation of **13**, where the higher electrophilicity of the cationic complex is crucial, promoting the attack even at a carbon atom of inner position. The increased concentration of HO^- , however, effectively shielded the cationic $\text{Mn}^{\text{V}}=\text{O}$ complex in such a reaction. These results are in accordance with recent observations regarding photogenerated $(\text{P})\text{Mn}^{\text{V}}=\text{O}$ complexes, the reactivity of which was significantly decreased by anionic axial ligands (on the opposite side of the coordinated O atom), due to the diminished electrophilicity [21]. Additionally, the $(\text{P})\text{Mn}^{\text{IV}}-\text{O}_2^{\bullet-}$ complex could

also promote the formation of the keto group at the outer position, according to Equations (4)–(7). Its reactivity, however, was also dramatically decreased by the axial coordination of a hydroxo ligand.

An increase in the concentration of dissolved O_2 , by application of oxygen saturation, caused dramatic enhancements in the product ratios with the anionic catalyst, compared to the cases of air saturation (Scheme 3). Changing the pH from 7 to 10, the ratio of the hydroxy derivative (**11**) increased by 46%, while that of the peroxy product (**12**) displayed a slight increase, contrary to the significant diminution in air-saturated system. These results suggest that an increase of the HO^- concentration resulted in opposite effects, the resultant of which depends on further conditions. In this case, the oxygenation processes depending on the O_2 concentration were much more facilitated than the interactions impeding these substitutions. Hence, also the $Mn^V=O$ species plays some, even if minor, role in the production of **11**, too, because its formation is promoted by higher O_2 concentration.



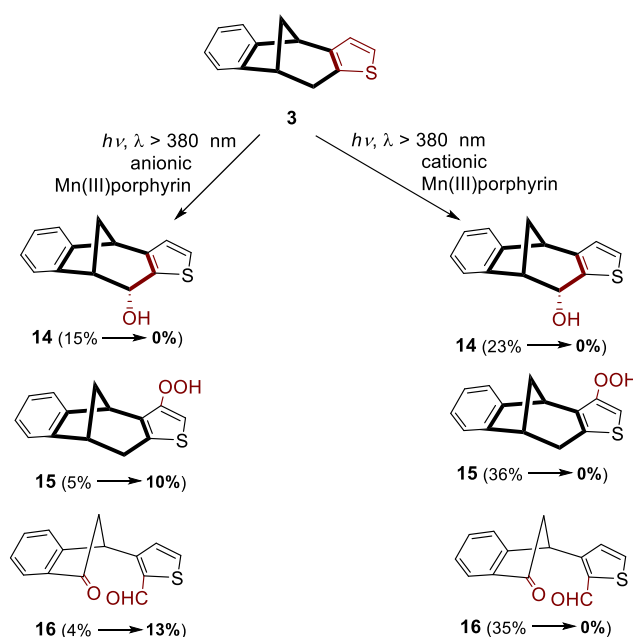
Scheme 3. Reaction pathways and product ratios for the photocatalytic oxygenation of **2** in oxygen-saturated systems. The arrows in parentheses indicate the change in the yields upon increasing the pH from 7 to 10.

In the case of the cationic catalyst, the tendency of the changes in the product ratios upon this pH increase remained the same at higher oxygen concentration, but with moderately higher enhancements (to 70% for **11** and to 10% for **12**). These results confirm the concept of the resultant of opposite effects. This is valid for the change in the ratio of product **13**. In that case, in accordance with the air saturated system, higher pH caused a dramatic decrease of the ratio to trace level, but from a 44% (due to the higher O_2 concentration). This observation indicates that the hampering, presumably shielding (of the positively charged complex) effect of the increased alkalinity is far predominant regarding the formation of **13**.

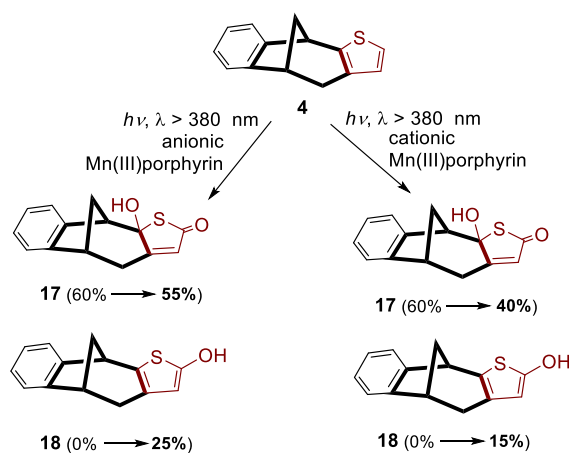
The changes caused by an increase in the HO^- concentration in the case of the thienyl derivatives considerably deviated from those observed for the corresponding furan compounds. For instance, the results obtained in aerated systems practically agreed with those observed in the oxygen-saturated solutions (see Schemes 4 and 5). Besides, the products formed from the thienyl derivative **5** significantly differed from those originated from the corresponding furyl compound (**1**), due to the more stable aromatic system in the previous one. Hence, in this case more oxidation reactions took place on carbon atoms out of the thiophene ring. Accordingly, in the case of the furan derivative **1** the products were functionalized exclusively at the carbon atoms originally belonging to the furan ring (via both substitution and ring cleavage), those formed from the corresponding thienyl compound possess the

oxygen-containing groups predominantly on the saturated hydrocarbon skeleton. However, the types of the two products of the other analogous thionyl (**4**) and furyl (**2**) isomers fully agreed.

The pH increase in the system with anionic photocatalyst led to the disappearance of the hydroxy derivative **14**, which is similar to the observation with the cationic one (Scheme 4). These results indicate that the $Mn^V=O$ species played the determining role in the production of this compound. However, the ratios of the products with higher oxygen content (peroxy and skeleton-cleaved keto-formyl derivatives, **15** and **16**, respectively) perceptively increased. These results are quite the opposite of those obtained with the cationic manganese(III) porphyrin, where none of these derivatives could be detected at pH = 10, while ratios of 35–36% were obtained at pH = 7. These phenomena suggest that the role of the $Mn^V=O$ species is crucial with the cationic complex, while hydroxyl radicals may be important with the anionic catalyst.



Scheme 4. Reaction pathways and product ratios for the photocatalytic oxygenation of **3** in air/oxygen-saturated systems. The arrows in parentheses indicate the change in the yields upon increasing the pH from 7 to 10.



Scheme 5. Reaction pathways and product ratios for the photocatalytic oxygenation of **4** in air/oxygen-saturated systems. The arrows in parentheses indicate the change in the yields upon increasing the pH from 7 to 10.

Like the 3-furyl derivative **2**, the photocatalytic oxygenation of the corresponding thienyl compound **4** at pH = 10 resulted in a product (**18**) that is hydroxylated at the outer carbon atom adjacent to the heteroatom of the aromatic ring (Scheme 5). However, the yield of this product increased from about 18–28% to 70% in the case of the furan derivative, while the corresponding thiophene product appeared only at the higher pH (=10). This phenomenon confirms that an increase of pH promotes this type of hydroxylation of both compounds with both catalysts, but the reactivity of the thienyl derivative is significantly less than that of the furyl type. Consequently, in accordance with the corresponding furyl derivative (**2**), hydroxyl radical is the main oxidative agent in this reaction, due to its favored production at higher pH.

Interestingly, compared to the furan compound **2**, the ratio of product **17** just moderately decreased upon increasing pH (from 7 to 10), while that of the corresponding hydroxy furanon product (**13**, formed only with the cationic catalyst) diminished to “traces”. These decreases confirm the determining role of the $Mn^V=O$ and partly the $(P)Mn^{IV}-O_2^{\bullet-}$ species in the formation of this type of product. However, the significantly higher product ratios for the thiophene product needs further considerations.

The yields and turnover numbers of the products obtained in the photocatalytic oxygenations of **2**, **3**, and **4** under various conditions are summarized in Table 1.

Table 1. The yields and turnover numbers (TON) of the products of photocatalytic oxygenations at various conditions.

Products	Yields (TON)							
	with Anionic Catalyst				with Cationic Catalyst			
	pH = 7 ^a		pH = 10		pH = 7 ^a		pH = 10	
from 2 ^b								
11	14%(156)	24%(252)	15%(167)	70%(820)	18%(217)	18%(190)	65%(747)	70%(805)
12	5%(58)	8%(88)	traces	10%(115)	5%(63)	5%(54)	8%(88)	10%(103)
13	0%	0%	0%	0%	27%(293)	44%(454)	traces	trace
from 3								
14	15%(160)		0%		23%(240)		0%	
15	5%(55)		10%(110)		36%(40)		0%	
16	4%(45)		13%(145)		35%(440)		0%	
from 4								
17	60%(645)		55%(630)		60%(660)		40%(450)	
18	0%		25%(290)		0%		15%(160)	

^a The values regarding pH = 7 were taken from previous works [18,20]. ^b The first value was obtained in aerated system, the second one in oxygen-saturated solution at a given catalyst-pH combination. (For substrates **3** and **4**, the same yields were obtained under both conditions.).

The structures of all of the obtained compounds **11–18** were confirmed by complete characterizations utilizing modern spectroscopic methods. The spectra were in accordance with those of the structures previously synthesized under different reaction conditions (including pH) [17,18,20]. All of these compounds have a specific pattern of aliphatic protons which is characteristic for the benzobicyclo[3.2.1]octadiene skeleton with different functionalities gained in the photooxygenation reactions. Functionalization of the 3-thienyl substituted benzobicyclo[3.2.1]octadiene **4** gave a new product, **18**, that is hydroxylated at position 5 of the furan ring. It has a pattern of protons in ¹H NMR that are distinguishable and differ from the pattern of the starting compound **4** (Figure 1). Here, the protons H_A-H_C and the proton of the OH group are situated in the region between 5.3 and 1.9 ppm. The synthesis of this kind of hydroxylated products is very difficult in thermal reactions and there is no procedure in the literature regarding the introduction of OH group onto the heteroaromatic (furan) ring. According to these facts, both hydroxylated products (**11** and **18**) are the most valuable ones as intermediates for further functionalization, the long-term goal of which is to increase the lipophilicity of all the new structures and to get better physico-chemical properties.

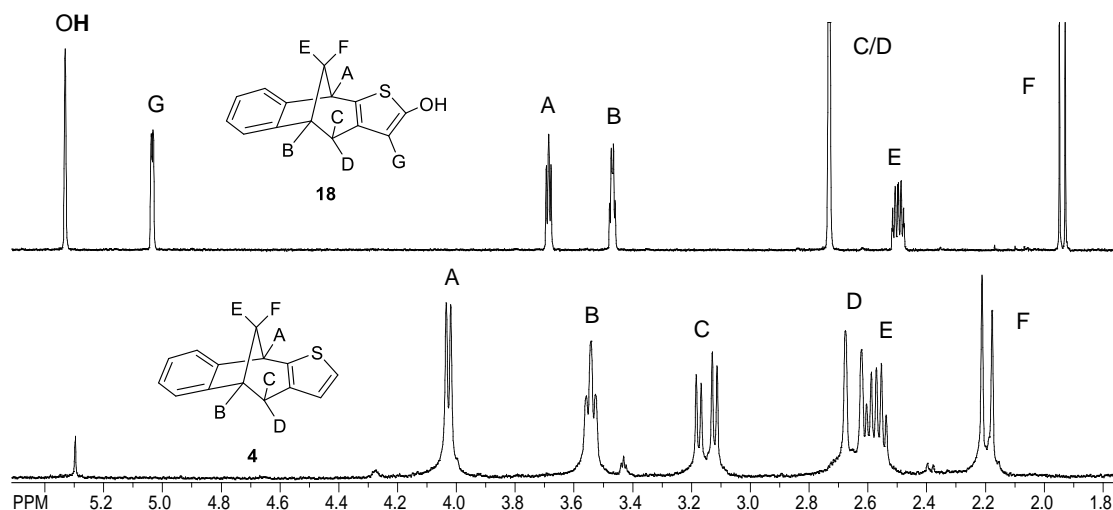
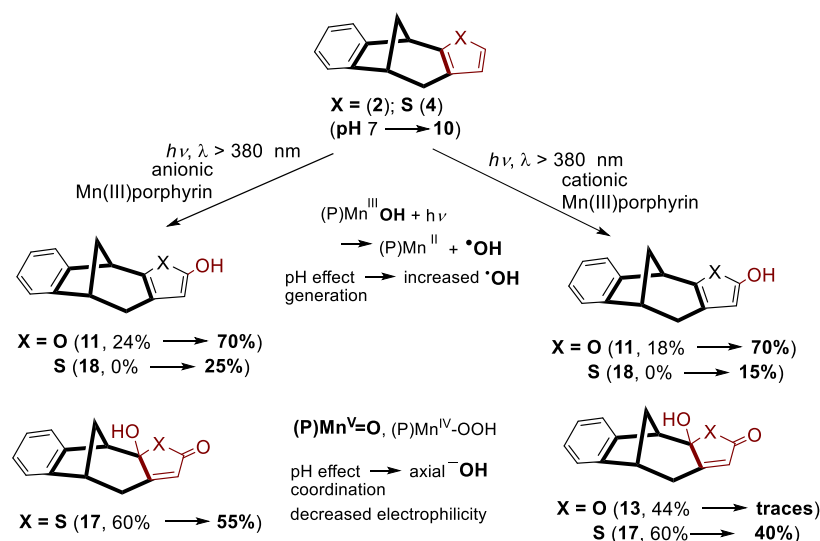


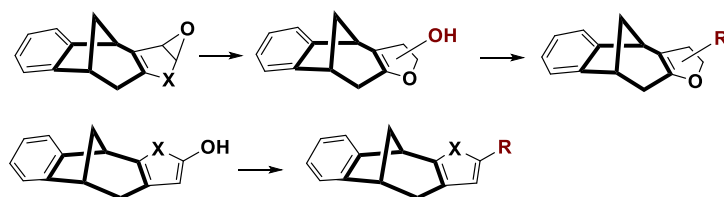
Figure 1. Comparison of the proton NMR spectra of the starting compound **4** and the photooxygenation product **18**.

Comparing the products and the changes of their yields obtained for the furan and thiophene derivatives oxygenated under various conditions, it is clearly seen that the products of the furan compound (**1**) and the analogous thiophene derivative (**3**) are totally different, due to the dramatic effect of the heteroatom on the ways of oxygenation. Accordingly, the effects of the pH increase cannot be interpreted by an overall scheme. However, the types of the main products in the case of substrates **2** and **3** well agree, hence, they properly demonstrate the effects of the pH change on their photocatalytically oxygenated derivatives. As shown in Scheme 6, in the oxygenation leading to the analogous products **11** and **18** the main oxidizing agent is hydroxyl radical, the formation of which is promoted by an increase of the HO^- concentration. Its reactions with the substrates cannot be affected by the charge of the photocatalyst. In the case of products **13** and **17**, however, the pH increase significantly diminished the yields obtained with the cationic catalyst, due to the axial coordination of a hydroxide ion, decreasing the electrophilicity of $(\text{P})\text{Mn}^{\text{V}}=\text{O}$, the main agent in these oxygenation reactions.



Scheme 6. Characteristic products of photocatalytic oxygenation of analogous furan and thiophene derivatives, indicating the oxidizing agents playing determining role in their formation. The arrows in parentheses indicate the change in the yields upon increasing the pH from 7 to 10.

Utilization of this type of photocatalytic oxygenation can also be applied for synthesis of other novel benzobicyclo[3.2.1]octadiene derivatives with oxygen or other functional groups, even more similar to natural structures, by their subsequent transformations as presented in Scheme 7.



Scheme 7. Further possible applications of the photocatalytic oxygenation products obtained by using Mn(III) porphyrins.

3. Materials and Methods

3.1. Materials

The compounds used in our experiments were of reagent grade. The cationic and anionic manganese(III) porphyrins as photocatalysts, (Mn(III)TMPyP⁵⁺) and (Mn(III)TSPP³⁻), respectively, were purchased from Frontier Scientific. The furyl and thienyl derivatives of benzobicyclo[3.2.1]octadiene (**2**, **3**, and **4**) were prepared according to the procedures previously described [22]. Organic solvents applied for the experiments were purified by distillation, while water was treated with a Millipore/Milli-Q system.

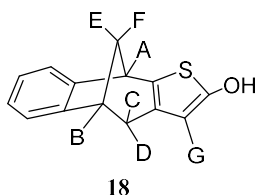
3.2. Experimental

3.2.1. General

The ¹H spectra were recorded on a spectrometer at 600 MHz. The ¹³C NMR spectra were registered at 150 MHz. All NMR spectra were measured in CDCl₃ using tetramethylsilane as reference. Silica gel (0.063–0.2 mm) was used for chromatographic purifications. Thin-layer chromatography (TLC) was performed silica gel 60 F₂₅₄ plates.

3.2.2. Typical Experimental Procedure for the Photocatalytic Oxygenation

50 cm³ solutions containing the starting substrates **2–4** (4×10^{-3} mol dm⁻³) and the anionic or cationic manganese(III)porphyrins (4×10^{-5} mol dm⁻³) in acetone/water (50:50) at pH 10 were irradiated with a 70-W tungsten halogen immersion lamp (Philips, $\lambda_{ir} > 380$ nm) in a thermostated 50-cm³ cylindrical photoreactor. Thus, the substrate/catalyst ratio (S/C) was 100 in all cases. A stream of air or oxygen (as a source of O₂) was passed through the solutions at RT during 8 h (compounds **2** and **4**) or 16 h (compound **3**), also ensuring a vigorous stirring. After termination of the photolysis acetone was removed by vacuum distillation. The remaining two phases were separated by standard methods. The water-insoluble oxygenation products remained in the organic phase. The photoproducts **11**, **12** and **13** from **2**, **14**, **15**, and **16** from **3**, **17** and **18** from **4** (see Schemes 2–5) were isolated by repeated thin-layer chromatography using dichloromethane/diethylether (9:1) as eluent and characterized by spectroscopic methods. The photoproducts **11–17** were identified and reported previously, with different yields at pH 7 [18,20], for comparison with the experiments at pH 10. The data for the new photooxygenation product **18** is given below.



3-thiatetracyclo[6.6.1.0^{2,6}.0^{9,14}]pentadeca-2(6),4,9,11,13-pentaen-7-ol (**18**): 25%, R_f 0.75 (dichloromethane/diethylether = 9:1); colourless oil; ^1H NMR (CDCl_3 , 600 MHz) δ 7.19 (d, $J = 7.3$ Hz, 1H), 7.10–7.16 (m, 3H), 5.32 (s, $-\text{OH}$, 1H), 5.03 (d, $J_{\text{G-OH}} = 2.5$ Hz, 1H), 3.77 (t, 1H, $J = 5.3$ Hz, H-A), 3.46 (dd, $J = 8.3; 4.1$ Hz, 1H, H-B), 2.70–2.74 (m, 2H, H-C, H-D), 2.45–2.51 (m, 1H, H-E), 1.93 (d, 1H, $J = 11.9$ Hz, H-F); ^{13}C NMR (CDCl_3 , 150 MHz) δ 167.9 (s), 144.8 (s), 139.7 (s), 127.9 (d), 127.4 (d), 125.0 (d), 122.6 (d), 118.0 (d), 82.8 (d), 46.4 (d), 41.8 (d), 40.7 (d), 35.4 (t); MS m/z : 228 (M^+ , 100%), 211 (60%); HRMS (Q-TOF LC/MS) for $\text{C}_{14}\text{H}_{12}\text{OS}$: ($\text{M} + \text{H}$)⁺ $_{\text{calcd}}$ 229.0635, ($\text{M} + \text{H}$)⁺ $_{\text{measured}}$ 229.0677.

Since the quantum yields could not be estimated in these photocatalytic experiments, due to the complicated product analysis hampering reliable kinetic measurements, the turnover numbers (TON) were calculated on the basis of the product yields and the consumption of the catalyst during the irradiation. Notably, the degradation of the catalyst did not exceed 10% in any of these experiments. The conversion of the starting substrate reached 100% in all cases.

4. Conclusions

As our results indicated, in most cases, the increase of pH from 7 to 10 significantly affected not only the yields of the products, but in several instances, it led to their total vanishing or, oppositely, to the appearance of a new one, depending on the type and position of the heteroatom in the aromatic moiety and the charge of the photocatalyst. Hence, the selectivity of the photocatalytic oxygenation of the furyl derivatives could be perceptively improved by this pH increase, e.g., the yield of compound **11** dramatically increased (from 18–24% to 70%) with both catalysts. The results obtained for the corresponding thienyl compounds, however, were different in this respect. The selectivity for the formation of compounds **15** and **16** (from **3** with anionic catalyst) was significantly enhanced, but an additional product (**18**) appeared in the case of **4**. These results clearly demonstrated that, regarding the systems studied, careful selections of pH, starting substance, and catalyst can promote considerable improvements in the selectivity of photooxygenation reactions. Besides, comparisons of the pH effects on the yields delivered important hints of the agents playing the main role in the oxygenation of the related products. Hence, hydroxyl radicals and (P) $\text{Mn}^{\text{V}}=\text{O}$ intermediates proved to be the determining oxidants.

Author Contributions: Conceptualization, I.Š. and O.H.; methodology, I.Š.; validation, D.V.; formal analysis, I.Š. and D.V.; investigation, I.Š. and D.V.; resources, I.Š. and O.H.; data curation, I.Š. and D.V.; writing—original draft preparation, I.Š. and O.H.; writing—review and editing, I.Š. and O.H.; supervision, I.Š.; project administration, I.Š.; funding acquisition, I.Š. and O.H.

Funding: This work was supported by the Széchenyi 2020 under the EFOP-3.6.1-16-2016-00015 and by grants from the University of Zagreb short term scientific support under the title Synthesis and functionalization of novel (hetero)polycyclic photoproducts for 2018.

Conflicts of Interest: The authors declare no conflict of interest.

References

- Hennig, H.; Lupp, D. Photocatalytic activation of oxygen by iron(III) porphyrins. *J. Für Prakt. Chem.* **1999**, *341*, 757–767. [[CrossRef](#)]
- Maldotti, A.; Andreotti, L.; Molinari, A.; Varani, G.; Cerichelli, G.; Chiarini, M. Photocatalytic properties of iron porphyrins revisited in aqueous micellar environment: Oxygenation of alkenes and reductive degradation of carbon tetrachloride. *Green Chem.* **2001**, *3*, 42–46. [[CrossRef](#)]

3. Funiyu, S.; Kinai, M.; Masui, D.; Takagi, S.; Shimada, T.; Tachibana, H.; Inoue, H. Key reaction intermediates of the photochemical oxygenation of alkene sensitized by RuII-porphyrin with water by visible light. *Photochem. Photobiol. Sci.* **2010**, *9*, 931. [[CrossRef](#)]
4. Shimada, T.; Kumagai, A.; Funiyu, S.; Takagi, S.; Masui, D.; Nabetani, Y.; Tachibana, H.; Tryk, D.A.; Inoue, H. How is the water molecule activated on metalloporphyrins? Oxygenation of substrates induced through one-photon/two-electron conversion in artificial photosynthesis by visible light. *Faraday Discuss.* **2012**, *155*, 145–163. [[CrossRef](#)] [[PubMed](#)]
5. Kalajahi, S.S.M.; Hajimohammadi, M.; Safari, N. Highly efficient, green and solvent-free photooxygenation of alkenes by air and visible light or sunlight in the presence of porphyrin sensitizers. *React. Kinet. Mech. Catal.* **2014**, *113*, 629–640. [[CrossRef](#)]
6. Zhang, R.; Vanover, E.; Luo, W.; Newcomb, M. Photochemical generation and kinetic studies of a putative porphyrin-ruthenium(v)-oxo species. *Dalton Trans.* **2014**, *43*, 8749–8756. [[CrossRef](#)] [[PubMed](#)]
7. Hajimohammadi, M.; Schwarzinger, C.; Knör, G. Controlled multistep oxidation of alcohols and aldehydes to carboxylic acids using air, sunlight and a robust metalloporphyrin sensitizer with a pH-switchable photoreactivity. *RSC Adv.* **2012**, *2*, 3257. [[CrossRef](#)]
8. Kurimoto, K.; Yamazaki, T.; Suzuri, Y.; Nabetani, Y.; Onuki, S.; Takagi, S.; Shimada, T.; Tachibana, H.; Inoue, H. Hydrogen evolution coupled with the photochemical oxygenation of cyclohexene with water sensitized by tin(IV) porphyrins by visible light. *Photochem. Photobiol. Sci.* **2014**, *13*, 154–156. [[CrossRef](#)] [[PubMed](#)]
9. Hennig, H. Homogeneous photo catalysis by transition metal complexes. *Coord. Chem. Rev.* **1999**, *182*, 101–123. [[CrossRef](#)]
10. Hajimohammadi, M.; Bahadoran, F.; Davarani, S.S.H.; Safari, N. Selective photocatalytic epoxidation of cyclooctene by molecular oxygen in the presence of porphyrin sensitizers. *React. Kinet. Mech. Catal.* **2009**, *99*, 243–250. [[CrossRef](#)]
11. Zhang, R.; Horner, J.H.; Newcomb, M. Laser Flash Photolysis Generation and Kinetic Studies of Porphyrin-Manganese-Oxo Intermediates. Rate Constants for Oxidations Effected by Porphyrin-Mn(V)-Oxo Species and Apparent Disproportionation Equilibrium Constants for Porphyrin-Mn(IV)-Oxo Species. *J. Am. Chem. Soc.* **2005**, *127*, 6573–6582. [[CrossRef](#)] [[PubMed](#)]
12. Newcomb, M.; Zhang, R.; Pan, Z.; Harischandra, D.; Chandrasena, R.; Horner, J.; Martinez II, E. Laser flash photolysis production of metal-oxo derivatives and direct kinetic studies of their oxidation reactions. *Catal. Today* **2006**, *117*, 98–104. [[CrossRef](#)]
13. Zhang, R.; Newcomb, M. Laser Flash Photolysis Generation of High-Valent Transition Metal–Oxo Species: Insights from Kinetic Studies in Real Time. *Acc. Chem. Res.* **2008**, *41*, 468–477. [[CrossRef](#)] [[PubMed](#)]
14. Hennig, H.; Behling, J.; Meusinger, R.; Weber, L. Photocatalytic Oxygenation of Selected Cycloalkenes in Aqueous Solutions Induced by Water-Soluble Metal Porphyrin Complexes. *Chem. Ber.* **1995**, *128*, 229–234. [[CrossRef](#)]
15. Baglia, R.A.; Zaragoza, J.P.T.; Goldberg, D.P. Biomimetic Reactivity of Oxygen-Derived Manganese and Iron Porphyrinoid Complexes. *Chem. Rev.* **2017**, *117*, 13320–13352. [[CrossRef](#)]
16. Jung, J.; Ohkubo, K.; Goldberg, D.P.; Fukuzumi, S. Photocatalytic Oxygenation of 10-Methyl-9,10-dihydroacridine by O₂ with Manganese Porphyrins. *J. Phys. Chem. A* **2014**, *118*, 6223–6229. [[CrossRef](#)] [[PubMed](#)]
17. Kikaš, I.; Horváth, O.; Škorić, I. Functionalization of the benzobicyclo[3.2.1]octadiene skeleton via photocatalytic and thermal oxygenation of a furan derivative. *Tetrahedron Lett.* **2011**, *52*, 6255–6259. [[CrossRef](#)]
18. Kikaš, I.; Horváth, O.; Škorić, I. Functionalization of the benzobicyclo[3.2.1]octadiene skeleton via photocatalytic oxygenation of furan and benzofuran derivatives. *J. Mol. Struct.* **2013**, *1034*, 62–68. [[CrossRef](#)]
19. Vuk, D.; Horváth, O.; Marinić, Ž.; Škorić, I. Functionalization of the benzobicyclo[3.2.1]octadiene skeleton possessing one isolated double bond via photocatalytic oxygenation. *J. Mol. Struct.* **2016**, *1107*, 70–76. [[CrossRef](#)]
20. Vuk, D.; Kikaš, I.; Molčanov, K.; Horváth, O.; Škorić, I. Functionalization of the benzobicyclo[3.2.1]octadiene skeleton via photocatalytic oxygenation of thiophene and furan derivatives: The impact of the type and position of the heteroatom. *J. Mol. Struct.* **2014**, *1063*, 83–91. [[CrossRef](#)]

21. Kwong, K.W.; Winchester, C.M.; Zhang, R. Photochemical generation of manganese(IV)-oxo porphyrins by visible light photolysis of dimanganese(III) μ -oxo bis-porphyrins. *Inorg. Chim. Acta* **2016**, *451*, 202–206. [[CrossRef](#)]
22. Vidaković, D.; Škorić, I.; Horvat, M.; Marinić, Ž.; Šindler-Kulyk, M. Photobehaviour of 2- and 3-heteroaryl substituted *o*-divinylbenzenes; formation of fused 2,3- and 3,2-heteroareno-benzobicyclo[3.2.1]octadienes and 3-heteroaryl benzobicyclo[2.1.1]hexenes. *Tetrahedron* **2008**, *64*, 3928–3934. [[CrossRef](#)]



© 2019 by the authors. Licensee MDPI, Basel, Switzerland. This article is an open access article distributed under the terms and conditions of the Creative Commons Attribution (CC BY) license (<http://creativecommons.org/licenses/by/4.0/>).